Vibrational Dynamics of Terminal Acetylenes: II. Pathway for Vibrational Relaxation in Gas and Solution

Hyun S. Yoo, Merrick J. DeWitt, and Brooks H. Pate*

Department of Chemistry, University of Virginia, McCormick Road, Charlottesville, Virginia 22904

Received: November 23, 2002; In Final Form: October 8, 2003

The pathway for vibrational-energy flow following the excitation of the first excited state of the acetylenic C−H stretch is investigated for a series of 10 terminal acetylenes in room-temperature gases and dilute solutions using transient absorption picosecond infrared spectroscopy. The transient absorption infrared spectra are obtained at three different probe frequencies. These experiments separately detect the population of the excited C−H stretch state, the population of vibrational states with 2 quanta of acetylenic C−H bend excitation, and the population of all other vibrational states with C−H stretch absorption frequencies within the laser bandwidth (25 cm^{-1}) of the C−H stretch fundamental frequency. These measurements show that the initial redistribution event for the isolated molecule involves population transfer to vibrational states with bend overtone excitation. The secondary intramolecular vibrational-energy redistribution (IVR) process, which involves population transfer to the remaining near-resonant vibrational states, occurs on a time scale that is about 5 times slower than the initial redistribution event. The same relaxation pathway is observed in dilute solution. The total relaxation rate in solution for the slower process can be quantitatively described using a simple model where IVR and solvent-induced vibrational-energy relaxation (VER) proceed independently. The main effects of the solvent are to increase the extent of population relaxation for the first stage of IVR and to cool vibrational excitation rapidly in the low-frequency acetylene wag normal-mode vibrations produced by the IVR dynamics.

Introduction

The flow of vibrational energy within a polyatomic molecule is a fundamental chemical process that underlies chemical reactivity.[1] At the most basic level, one would like to know the time scale for energy localization in a single vibrational mode following selective laser excitation.[2−7] For gas-phase systems, the relaxation rate of the isolated molecule can be measured by several techniques that use either frequency-[8,9] or time-domain[10−13] spectroscopy. In solution, frequency-domain techniques are largely inapplicable, and time-domain spectroscopy is the method of choice for measuring the vibrational-energy relaxation rate.[14−21] The application of time-resolved infrared spectroscopy to the measurement of the initial vibrational relaxation rate of the acetylenic C−H stretch fundamental was described in the previous paper.[11] (The application of frequency-domain techniques will be described in the following paper.[22]) The comparison of gas- and solution-phase measurements for a series of terminal acetylenes showed that a simple model for the total solution relaxation rate is obeyed to good accuracy.[11] The total solution-phase relaxation rate is the sum of a molecule-dependent rate, given by the fast relaxation component measured in the gas-phase experiments, and a molecule-independent rate that is attributed to solvent-assisted vibrational-energy relaxation (VER).[23−25] However, the previous measurements detected only the population of the initially prepared acetylenic C−H stretch excited state and cannot provide direct information on the pathway or mechanism of the relaxation process. In this paper, we employ two-color picosecond infrared spectroscopy to study the intramolecular vibrational-energy redistribution (IVR) pathway in the gas phase and the effects that solvation has on these dynamics.

Much of the recent work in the field of intramolecular vibrational dynamics has been focused on developing methods that use laser excitation to affect the outcome of chemical reactions.[26] Most of the work in this field involves isolated molecules in the gas phase because the complications of solvent interactions are not present. Still, the control of chemical reactions with light in the solution phase is considered the ultimate goal.[27] The simplest and earliest proposal for laser chemistry is to enhance the reactivity at a specific bond site through the coherent excitation of a localized vibrational mode (e.g., a hydride stretch). The success of this approach requires the vibrational energy to remain localized for the time scale of the reaction (e.g., the mean collision time for a bimolecular reaction). Knowledge of the relaxation rate makes it possible to assess the feasibility of this approach. The ability to perform bond-selective chemistry with lasers has been demonstrated for small molecules in the gas phase.[28−34] In these systems, IVR does not occur because of the lack of an intramolecular vibrational bath of sufficient density.[9,35] Many experimental studies have shown that the initial time scale for energy relaxation is too fast to expect this simple approach to succeed in large polyatomic molecules. Furthermore, the new energy relaxation processes introduced by solvation can cause rapid vibrational-energy relaxation even for small molecules.[14,36,37] In general, the extension of direct mode-selective chemistry schemes to large molecules or to the solution phase faces significant physical limitations.

* Corresponding author. E-mail: bp2k@virginia.edu.

10.1021/jp027546n CCC: $27.50
Published on Web 01/31/2004

The poor prospects of success for bond-selective chemistry have spurred the development of new approaches to laser chemistry based on coherent control of the molecular motion.[26,38−40] These approaches fall roughly into two categories: active and passive control. The active-control approaches use strong laser fields to dictate the molecular motion through the molecule−field interaction.[38] Detailed knowledge of the molecular Hamiltonian is required to unlock the full potential of this approach. This level of understanding of the Hamiltonian for a large molecule, especially at reactive energies, remains a formidable problem in molecular spectroscopy.[41] The extension of adaptive learning algorithms can bypass this requirement[42] and have shown impressive initial success for simple reactions of large molecules.[43,44] Significant challenges exist for extending this approach to coherent control to the solution phase. For example, it will be important to know the time scale for maintaining intramolecular coherence in solution to translate this approach to solvated molecules.

Passive-control techniques propose using lasers in concert with the underlying intramolecular dynamics.[26,40,45] In this approach, coherent excitation creates an initial wave packet that subsequently evolves on the intramolecular potential energy surface. The molecule can then be intercepted at some point along the reaction pathway by a second time-delayed laser pulse. The spectral properties of this pulse (e.g., delay time and frequency) can be used to influence the molecular dynamics. The basic concepts in this approach to laser chemistry could possibly survive the transition from isolated- to solvated-molecule conditions in a robust manner. For example, the existence of a well-defined relaxation pathway does not require the maintenance of full quantum coherence.[46,47] This principle is well known in the field of multiphoton spectroscopy.[48−50] In the absence of coherence, the dynamics can be described using simple kinetics models through a set of master equations. For dynamics occurring on distinct time scales, the relaxation pathway is preserved, leaving open the possibility of intercepting the molecule at an opportune time.

Energy removal from the molecule by the solvent provides an additional complication but could be potentially useful. An example of this idea is the use of lasers to manipulate the geometry of a polyatomic molecule as it moves along the isomerization pathway. Because the normal-mode frequencies depend on the molecular structure, reaction control can be obtained through frequency selectivity of the laser pulses. The basic principle of this type of laser chemistry has been demonstrated for reasonably large polyatomic molecules using infrared multiphoton excitation.[51−53] In these experiments, collisional-energy relaxation is essential to stabilizing the new isomers. If an isomerization reaction involving several geometries follows a sequential reaction kinetics scheme, then product selectivity can be achieved by properly "timing" the collisional relaxation time (by the variation of solvent density in a supercritical fluid or possibly by using solvents that show a preferential interaction with the different isomers).[54] Exercising control over the isomeric structure could be used to affect the product distribution of subsequent reactions where a well-defined nuclear arrangement is required for reaction (e.g., Diels−Alder and other electrocyclic reactions).[55]

For both a fundamental understanding of chemical reactions and the development of laser chemistry methods, knowledge of the relaxation pathway for intramolecular dynamics is essential. For the fastest dynamical events (<1 ps), conventional spectroscopy techniques (e.g., FTIR spectroscopy) are well suited.[56,57] Spectroscopic assignment of the perturbed spectrum, often with the support of ab initio calculations,[41] can be used to obtain the key terms in the molecular Hamiltonian that control the early-time dynamics. For longer time scales, traditional spectroscopic analysis methods become difficult, especially for large molecules. On these time scales, there are many interacting vibrational states. An accurate analysis of the spectrum in terms of the normal modes would likely require significant guidance from ab initio calculations, but current electronic structure calculations lack the necessary accuracy. Theoretical techniques that work at a more "coarse-grained" level can provide an important qualitative understanding of the dynamics on these time scales.[58,59]

In this secondary range of time scales (>1 ps), experimental methods that can elucidate the reaction pathway become especially important, and significant advances have been achieved using time-domain vibrational spectroscopy to examine dynamics on this time scale. These techniques measure the time evolution of the vibrational spectrum following initial coherent excitation. Perhaps the most powerful technique is time-resolved infrared−Raman spectroscopy, which has been used to study vibrational-energy relaxation in solution.[60−63] For small polyatomic molecules, it has recently been possible to monitor the vibrational population in all of the normal modes.[62−65] Sensitivity improvements are needed to extend this technique to gas-phase samples. Two-color infrared spectroscopy offers improved sensitivity and can be used to study gas-phase samples, as shown in this paper. As discussed below, there are some limitations to using infrared spectroscopy that make this method less attractive than the Raman spectroscopy methods.[66] However, in favorable cases important information about the vibrational relaxation pathway can be obtained. Other time-domain techniques that provide information about the relaxation pathway have been developed and may be applicable to gas-phase systems. Most notably, the combination of picosecond infrared excitation and fluorescence spectroscopy probing offers high sensitivity and has already been successfully applied to the low-density environment of molecular beams.[67]

Experimental Section

The results from three different transient absorption spectra are analyzed for both isolated (room-temperature gases) and solvated molecules. The study includes 10 terminal acetylenes in 5 solvents and as a room-temperature gas (a total of 180 transient absorption spectra). The experimental details for these two-color picosecond experiments and a listing of the molecules and solvents are provided in the previous paper.[11] For all three measurements, a strong infrared pump pulse (10 μJ/pulse, 1.4-ps pulse duration) is used to populate the first excited state of the acetylenic C−H stretch through the fundamental absorption ($v = 0 - v = 1$). The pump frequency is the same for all terminal acetylenes. For the gas-phase samples, this frequency is 3330 cm^{-1}. In dilute solution (0.05 M), the fundamental is shifted to lower frequency (for example, to 3310 cm^{-1} in CCl_4 solution; for the other solvents, please see Appendix D of the previous paper[11]). A second weaker pulse (0.4 μJ/pulse, 1.4-ps pulse duration) is used to measure the transient absorption spectrum. The two laser pulses have a relative polarization angle of 54.7° (magic angle) to remove rotational reorientation effects from the signals. The absorption of the full bandwidth of the laser pulse (25 cm^{-1}) is measured to obtain the transient absorption spectrum.

The three transient absorption measurements differ in the frequency of the probe laser. The population of the excited C−H stretch is directly monitored in one experiment by probing the $v = 1-v = 2$ excited-state absorption. The frequency of this absorption is shifted by -105 cm^{-1} by the diagonal anharmonicity of the C−H stretch. This shift is the same for both gas- and solution-phase samples, showing that the molecular anharmonic constants are unaffected by solvation. When compared to the other measurements in this study, the factor-of-2 increase in the transition moment in the harmonic oscillator limit must be considered when relating the absorption strength to the excited-state population. These measurements were presented in the previous paper where the data and its analysis are described.[11]

In the second measurement, the frequency of the probe laser is shifted -40 cm^{-1} from the fundamental frequency. Absorption at this frequency directly probes the population of vibrational states that contain 2 quanta of the acetylenic C−H bend. This frequency shift is also the same for gas and solution samples. Because this shift is larger than the frequency bandwidth of the laser, this signal is obtained with almost no "leakage" of absorption at either the C−H fundamental or excited-state absorption frequencies. Therefore, as in the excited-state absorption measurement, this signal provides a direct measure of the population of the bend overtone states. The transition that gives rise to this signal is a fundamental in the C−H stretch normal mode, so its transition strength is expected to be half as strong as the excited-state absorption.

The third transient absorption measurement uses a probe frequency at the C−H stretch fundamental frequency (effectively a single-color experiment). The interpretation of the transient absorption signal at this probe frequency is more complicated than for the previous two cases. The signal at this frequency contains two contributions: a stimulated emission pumping (SEP) signal and a ground-state bleach signal.[10,66] The transition strength associated with each of these components is that of the C−H stretch fundamental. Therefore, at $t = 0$ there are two signal contributions of equal magnitude that are proportional to the excited-state population. Because each contribution is proportional to the transition strength of the fundamental, the magnitude of the transient absorption signal at this probe frequency is the same as the transient absorption signal when the $v = 1-v = 2$ excited-state absorption is probed.

The SEP signal is directly related to the excited-state population and leads to increased transparency of the sample. The time dependence of this term is the same as the excited-state absorption signal measured when the $v = 1-v = 2$ transition is probed. The second contribution has a time dependence that reflects the recovery of absorption at the fundamental frequency (i.e., the bleach recovery). This part of the signal also leads to increased transparency and recovers whenever vibrational states with small anharmonic shifts of the C−H stretch fundamental (less than the laser bandwidth) are populated.[66] The recovery of this signal does not imply that the molecule has lost its energy and returned to the ground vibrational state. Therefore, a bleach recovery is observed for the isolated molecule despite the fact that the total vibrational energy in the molecule remains constant.[10]

For terminal acetylenes, the only normal mode that will not contribute to the bleach-recovery part of the signal when it is populated is the acetylenic C−H bend. For example, if vibrational states with bend overtone excitation comprise the first stage of the relaxation process, then a biexponential signal will be observed when the C−H stretch fundamental frequency is probed. The SEP contribution will have a time constant determined by the lifetime of the C−H stretch excited-state population decay into the set of vibrational states with bend overtone excitation. However, energy flow into these states will not accomplish the recovery of the bleach term. Instead, this part of the signal will have a time constant given by the decay of the bend overtone states into other normal modes with small anharmonic shifts. The observation of biexponential bleach-recovery signals is often said to reflect a "bottleneck" in the vibrational dynamics.[68,69] This bottleneck behavior is a common feature in the transient absorption spectra of the terminal acetylenes.

Results

The three two-color infrared spectroscopy measurements described above have been performed on both room-temperature gas and dilute solution samples. The analysis of these measurements is described below.

Analysis of Solution Measurements. The solution-phase transient absorption spectra can be quantitatively fit to simple single-exponential and biexponential forms. The kinetics model and analytical expressions for the transient absorption signals are presented in Appendix A. As described in the discussion of Appendix A, the two time scales that appear in the spectra correspond to the total relaxation rate of the first excited state of the acetylenic C−H stretch and the relaxation rate of the vibrational states with 2 quanta of acetylenic C−H bend excitation that are populated in the initial C−H stretch relaxation process. The C−H stretch relaxation rate is observed in three places: (1) the single-exponential decay of the excited-state absorption signal, (2) the rise in absorption at the characteristic frequency of vibrational states with bend overtone excitation (-40-cm^{-1} shift from the C−H stretch fundamental), and (3) the SEP contribution to the absorption recovery at the fundamental frequency. The relaxation rate of the bend overtone vibrational states appears in both the fall rate of the bend overtone absorption signal and the bleach-recovery signal obtained at the frequency of the acetylenic C−H stretch fundamental.

The three transient absorption measurements for tertbutylacetylene in dilute CCl_4 solution are shown in Figure 1. The excited-state absorption measurements for the 10 terminal acetylenes in dilute solution were analyzed in the previous paper.[11] The set of transient absorption spectra with the fit results for the set of terminal acetylenes in CCl_4 solution is shown in Appendix A. Experimental results for two molecules in all five solvents are also shown in Appendix A to illustrate the measurement signal-to-noise ratio in different solvents and the quality of the data fits using simple single-exponential or biexponential functional forms. The lifetimes of the initial C−H stretch relaxation and the relaxation of vibrational states with bend overtone excitation in the five solvents are reported in Tables 1−5. Additional details of the data analysis for dilute solution can be found in Appendix A.

Analysis of Room-Temperature Gas-Phase Measurements. In the previous paper, we showed that the population relaxation of the first excited state of the acetylenic C−H stretch has a biexponential form for most of the terminal acetylenes in the gas phase.[11] Two explanations for this result—populations with different IVR rates (proposed to be vibrational states with either

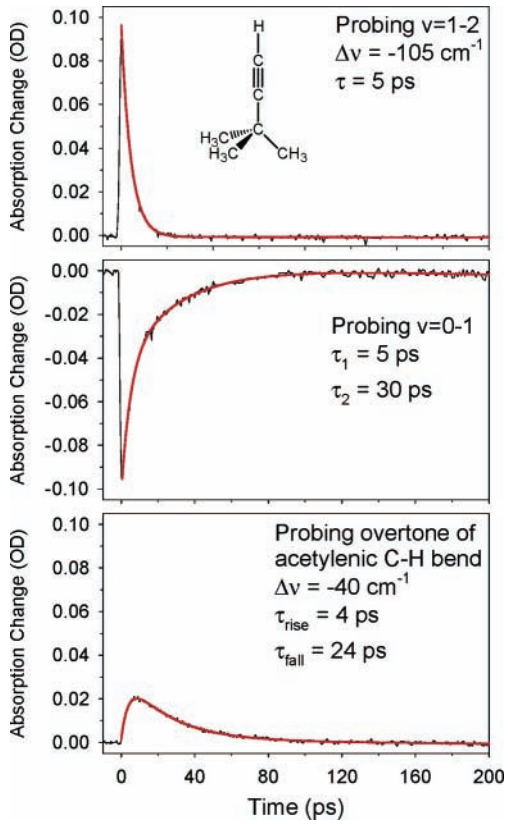

Figure 1. Three time-domain spectra of TBA in dilute CCl_4 solution. Decay of the excited-state absorption is described well with a single time constant shown in the top panel ($v = 1-v = 2$ probe measurement). The bleach-recovery signal shows a biexponential form (middle panel), indicating that the relaxation follows the indirect pathway (via the C−H bend overtone states). The fast component matches the time scale of the excited-state decay (probing $v = 1-v = 2$), and the slow component indicates the decay time of the bend overtone states. The transient absorption signal at the frequency region with bend overtone excitation (-40 cm^{-1}) is shown in the bottom panel, where the rise time indicates the time scale of the energy flow from the C−H stretch to vibrational states in the first tier and the fall time measures the time scale of the first-tier-state relaxation process. The two time constants measured in this frequency region match well with the two time constants obtained with the bleach-recovery signal.

1 or no quanta in the low-frequency acetylene wag) and an IVR process that occurs with two distinct time scales—were considered. The existing spectroscopic evidence favored the latter explanation, which is supported by the present measurements. The interpretation of the three two-color transient absorption measurements is performed using a tier model for the IVR process in terminal acetylenes. (See Figure A11 and the related discussion in ref 11.)

The initial IVR step involves rapid energy redistribution into a set of near-degenerate vibrational states that have 2 quanta of excitation in the acetylenic C−H bend normal mode. With 2 quanta of excitation in the bend, the acetylenic C−H stretch absorption frequency shifts -40 cm^{-1}. In the second stage of the IVR process, the energy is further redistributed from vibrational states with bend overtone excitation to vibrational states that have 1 or no quanta in the bend. The model also includes the possibility of direct relaxation of the C−H stretch into the dense set of vibrational states with 1 or no quanta of bend excitation. However, an analysis of the high-resolution molecular-beam infrared spectrum of methylbutenyne suggests that this pathway is slow compared to the tiered population flow through vibrational states with bend overtone excitation.[70] Using a random matrix model for the dynamics, the time-dependent populations in each tier following the initial preparation of the C−H stretch are shown in Figure 2. The populations of each tier are calculated by projecting the time-evolving coherent state into each of the basis states of the model Hamiltonian and then summing these probabilities for all basis states in the tier.[71] The parameters for the simulation are given in the previous paper (Figure A11 in ref 11).

The transient absorption intensity when the probe is shifted -40 cm^{-1} from the C−H stretch normal-mode frequency will be proportional to the population of the first-tier vibrational states. This population will not contribute to the bleach-recovery portion of the signal measured with the laser at the C−H stretch fundamental frequency. If the tier-model explanation is valid, then the transient absorption signal is expected to rise on the fast time scale of the IVR process and fall on the slower IVR time scale. As population builds up in the second tier, the transient absorption from this tier will contribute to bleach recovery in proportion to the total second-tier population. The bleach-recovery part of the signal should show this single time constant (although the SEP contribution contains both time scales).

However, full recovery of the initial bleach is not guaranteed even after the IVR process is complete. Following full IVR, the molecule can be expected to statistically populate the full set of near-resonant vibrational states. The normal-mode population characteristics of the near-resonant vibrational bath can be described with good accuracy by an effective temperature, T^*.[72,73] As the size of the molecule increases, the effective temperature is lowered, reflecting the fact that the vibrational bath has a larger heat capacity. For example, the value of T^* for butyne at 3330 cm^{-1} is approximately 544 °C. For TBA, the effective temperature is 274 °C. The absorption spectrum of the hot molecule is shifted and broadened by the off-diagonal

TABLE 1: Lifetimes (ps) of the Relaxation Process in Dilute CCl_4 Solution Measured at Three Different Frequencies[a]

molecule	τ (1−2)	τ_{fast} (0−1)	τ_{slow} (0−1)[b]	τ_{rise} (-40 cm^{-1})	τ_{fall} (-40 cm^{-1})
H−C≡CCH$_3$	22(2.2)	17(1.7)	80(19)	22(2.2)	70(7.0)
H−C≡CCH$_2$F	36(3.6)	50(5.0)		30(4.4)	46(8.7)
H−C≡CCH$_2$Cl	51(5.1)	67(6.7)		37(15)	64(25)
H−C≡CCH$_2$CH$_3$	7.8(0.8)	6.7(1.4)	27(2.7)	6.0(0.6)	32(24)
H−C≡CC(CH$_3$)=CH$_2$	3.6(0.5)	3.6(0.8)	25(3.9)	2.7(0.5)	22(2.2)
H−C≡CCH(CH$_3$)$_2$	5.7(0.6)	4.9(1.0)	20(2.6)	3.9(0.5)	21(2.1)
H−C≡CCHFCH$_3$	13(1.3)	11(1.2)	33(3.3)	9.5(1.5)	32(3.3)
H−C≡CCH$_2$CH$_2$F	23(2.3)	17(7.9)	35(6.1)	10(1.0)	72(9.6)
H−C≡CC(CH$_3$)$_3$	5.1(0.5)	5.3(0.5)	33(4.9)	4.0(0.5)	24(2.4)
H−C≡CSi(CH$_3$)$_3$	44(4.4)	53(7.8)		19(2.8)	210(190)

[a] Uncertainties are shown in parentheses. [b] Some of the $v = 0-v = 1$ probe measurements do not require the second time constant for the exponential fit to the decay spectrum, and no τ_{slow} value is reported for such cases.

TABLE 2: Lifetimes (ps) of the Relaxation Process in Dilute $CHCl_3$ Solution Measured at Three Different Frequencies[a]

molecule	τ (1−2)	τ_{fast} (0−1)	τ_{slow} (0−1)[b]	τ_{rise} (−40 cm^{-1})	τ_{fall} (−40 cm^{-1})
H−C≡CCH_3	17(1.7)	19(2.0)		8.1(2.2)	39(3.9)
H−C≡CCH_2F	33(3.3)	42(4.2)		19(4.5)	51(25)
H−C≡CCH_2Cl	41(4.1)	45(5.0)		20(6.5)	30(15)
H−C≡CCH_2CH_3	7.7(0.8)	7.3(3.7)	16(1.9)	5.2(0.5)	17(1.7)
H−C≡$CC(CH_3)$═CH_2	3.9(0.5)	4.5(1.9)	12(1.2)	1.9(0.5)	12(1.2)
H−C≡$CCH(CH_3)_2$	5.3(0.5)	4.8(0.5)	13(1.3)	2.9(0.5)	13(1.3)
H−C≡$CCHFCH_3$	14(1.4)	18(1.8)		12(5.0)	16(7.7)
H−C≡CCH_2CH_2F	23(2.3)	24(2.4)		7.2(0.7)	49(8.0)
H−C≡$CC(CH_3)_3$	4.9(0.5)	4.4(3.7)	17(1.7)	3.6(0.5)	14(1.6)
H−C≡$CSi(CH_3)_3$	39(3.9)	43(7.0)		24(4.4)	250(150)

[a] Uncertainties are shown in parentheses. [b] Some of the $v = 0-v = 1$ probe measurements do not require the second time constant for the exponential fit to the decay spectrum, and no τ_{slow} value is reported for such cases.

TABLE 3: Lifetimes (ps) of the Relaxation Process in Dilute $CDCl_3$ Solution Measured at Three Different Frequencies[a]

molecule	τ (1−2)	τ_{fast} (0−1)	τ_{slow} (0−1)[b]	τ_{rise} (−40 cm^{-1})	τ_{fall} (−40 cm^{-1})
H−C≡CCH_3	15(1.5)	16(1.6)		5.4(5.4)	25(4.7)
H−C≡CCH_2F	32(3.2)	34(3.4)		25(23)	25(23)
H−C≡CCH_2Cl	42(4.2)	42(4.2)		18(16)	300(270)
H−C≡CCH_2CH_3	7.8(0.8)	6.7(0.7)		3.5(0.5)	17(1.7)
H−C≡$CC(CH_3)$═CH_2	3.3(0.5)	2.1(0.5)	8.6(0.9)	2.1(0.5)	13(0.5)
H−C≡$CCH(CH_3)_2$	5.4(0.5)	7.4(0.7)		2.7(0.5)	11(2.6)
H−C≡$CCHFCH_3$	14(1.4)	16(1.6)		7.4(6.5)	8.9(8.0)
H−C≡CCH_2CH_2F	19(1.9)	24(2.4)		6.3(0.8)	17(15)
H−C≡$CC(CH_3)_3$	4.5(0.5)	3.4(0.5)	9.2(1.8)	4.0(1.1)	7.7(2.1)
H−C≡$CSi(CH_3)_3$	30(3.0)	41(4.1)		38(34)	38(34)

[a] Uncertainties are shown in parentheses. [b] Some of the $v = 0-v = 1$ probe measurements do not require the second time constant for the exponential fit to the decay spectrum, and no τ_{slow} value is reported for such cases.

TABLE 4: Lifetimes (ps) of the Relaxation Process in Dilute CH_2Cl_2 Solution Measured at Three Different Frequencies[a]

molecule	τ (1−2)	τ_{fast} (0−1)	τ_{slow} (0−1)[b]	τ_{rise} (−40 cm^{-1})	τ_{fall} (−40 cm^{-1})
H−C≡CCH_3	17(1.7)	16(3.0)		11(1.1)	30(6.5)
H−C≡CCH_2F	30(3.0)	34(3.4)		18(16)	23(21)
H−C≡CCH_2Cl	34(3.4)	33(3.3)		17(11)	25(23)
H−C≡CCH_2CH_3	6.7(0.7)	4.9(1.1)	16(1.6)	8.0(4.3)	11(6.9)
H−C≡$CC(CH_3)$═CH_2	3.6(0.5)	2.4(0.5)	13(1.3)	2.9(0.5)	15(1.5)
H−C≡$CCH(CH_3)_2$	5.2(0.5)	4.8(0.5)	16(1.6)	3.1(0.5)	19(2.1)
H−C≡$CCHFCH_3$	14(1.4)	18(1.8)		7.8(7.0)	8.9(8.0)
H−C≡CCH_2CH_2F	16(1.6)	22(2.2)		9.3(2.5)	19(17)
H−C≡$CC(CH_3)_3$	4.9(0.5)	2.7(0.5)	11(1.1)	3.2(0.5)	22(1.7)
H−C≡$CSi(CH_3)_3$	31(3.1)	15(2.1)	82(16)	33(30)	33(30)

[a] Uncertainties are shown in parentheses. [b] Some of the $v = 0-v = 1$ probe measurements do not require the second time constant for the exponential fit to the decay spectrum, and no τ_{slow} value is reported for such cases.

TABLE 5: Lifetimes (ps) of the Relaxation Process in Dilute CCl_3CN Solution, Measured at Three Different Frequencies[a]

molecule	τ (1−2)	τ_{fast} (0−1)	τ_{slow} (0−1)[b]	τ_{rise} (−40 cm^{-1})	τ_{fall} (−40 cm^{-1})
H−C≡CCH_3	21(2.1)	11(3.2)	100(38)	11(3.2)	73(7.3)
H−C≡CCH_2F	30(3.0)	48(4.8)		29(8.7)	48(26)
H−C≡CCH_2Cl	33(3.3)	48(4.8)		30(5.7)	48(4.8)
H−C≡CCH_2CH_3	6.8(0.7)	4.6(0.5)	26(2.6)	6.1(0.6)	32(3.2)
H−C≡$CC(CH_3)$═CH_2	3.7(0.5)	3.5(0.5)	22(2.2)	3.3(0.5)	26(2.6)
H−C≡$CCH(CH_3)_2$	4.4(0.5)	4.1(0.7)	24(2.4)	4.0(0.5)	27(2.7)
H−C≡$CCHFCH_3$	14(1.4)	19(4.0)		16(4.6)	23(9.3)
H−C≡CCH_2CH_2F	17(1.7)	27(2.7)		18(2.0)	32(6.2)
H−C≡$CC(CH_3)_3$	4.5(0.5)	3.4(0.5)	22(2.2)	4.5(0.5)	22(2.2)
H−C≡$CSi(CH_3)_3$	38(3.8)	41(4.1)	200(52)	31(14)	52(19)

[a] Uncertainties are shown in parentheses. [b] Some of the $v = 0-v = 1$ probe measurements do not require the second time constant for the exponential fit to the decay spectrum, and no τ_{slow} value is reported for such cases.

anharmonic terms in the Hamiltonian.[74,75] For the terminal acetylenes, population of the acetylenic C−H bend and acetylenic wag normal modes provides the major contributions to the shape of the hot-molecule spectrum.[76]

The two time-domain measurements for TBA are shown in Figure 3. The population of the C−H stretch excited state shows two relaxation time constants in the $v = 1-v = 2$ probe measurement: 6 and 39 ps. The rise of the transient absorption for vibrational states with overtone excitation in the C−H bend has the same time constant as the fast component of the excited-state population decay. The observation of population transfer to vibrational states with 2 quanta of C−H bend on this fast time scale provides strong experimental support for a tier-model explanation of the biexponential C−H stretch dynamics. For

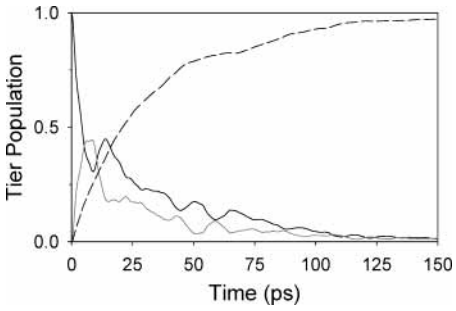

Figure 2. Time-dependent population change of each tier in the tier model (Figure A11 of ref 11). Following the initial excitation of the acetylenic C−H stretch, the excited-state population (black line) decays biexponentially as explained in Figure A14 of ref 11. The first-tier population rises as the energy is redistributed from the acetylenic C−H stretch. The time scale of the first-tier population rise rate matches the time constant of the fast component of the C−H stretch relaxation process. The first-tier population decays as the population is further distributed into the dense set of vibrational states (gray line). The second-tier population (dashed line) gradually rises as the energy is redistributed from both the actylenic C−H stretch and the first tier. This time scale matches both the slow component of the C−H stretch population decay and the decay of the first-tier population.

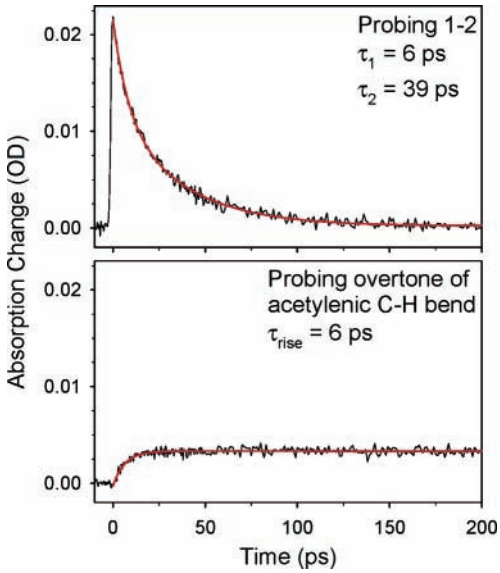

Figure 3. Two time-domain spectra of gas-phase TBA. The population of the C−H stretch excited state decays biexponentially in the $v = 1-v = 2$ probe measurement. The rise of the transient absorption for the vibrational states with the C−H bend overtone excitation (probing 40 cm^{-1} from the fundamental acetylenic C−H stretch frequency) has the same time constant as the fast component of the excited-state population decay. The tier-model explanation for the biexponential decay of the C−H stretch is supported by the observation of population transfer to the vibrational states with two quanta of C−H bend excitation.

this molecule, the bend overtone absorption amplitude remains relatively constant for longer times and does not fall as expected on the basis of the population dynamics in Figure 2.

To understand the behavior of the transient absorption signal in the bend overtone absorption region, we have measured the absorption spectrum at three time delays. These spectra are shown in Figure 4. At a time delay equal to the fast-component lifetime, a weak absorption feature appears that is peaked at the position expected for vibrational states with 2 quanta of C−H bend (−40 cm^{-1}). At a long time delay, after the excited-state population has completely decayed, a broad absorption spectrum is observed that tails off to low frequency. This is the absorption

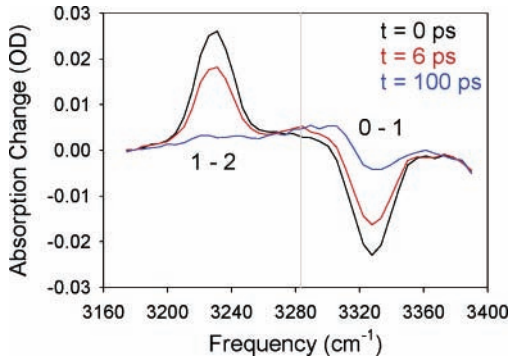

Figure 4. Transient absorption spectra of gas-phase TBA taken at three different delay times; at $t = 0$, at $^1/_e$ time of the IVR decay, and at long time. At $^1/_e$ time of the fast component of the IVR decay (6 ps), a weak absorption feature, peaking around −40 cm^{-1} from the C−H stretch fundamental frequency, appears, indicating that vibrational states with C−H bend overtone excitation are populated. The absorption spectrum of the hot molecule is shown at a long time delay after the excited-state population is completely redistributed. Although there is no peak at the bend overtone frequency region, the total absorption cross section of the vibrationally hot molecule at the frequency of states with bend overtone excitation (−40 cm^{-1}) is about the same as the one at the 6-ps delay, causing the nearly constant absorption at the fixed frequency offset of −40 cm^{-1} as shown in Figure 3.

spectrum of the hot molecule.[74,75] Although there is no peak at the bend overtone frequency, the total absorption cross section 40 cm^{-1} below the fundamental frequency is nearly the same at long time as it was at the 6-ps delay. This constancy of the absorption cross section, even while the overall shape of the absorption spectrum continues to evolve in time, causes the nearly constant absorption in Figure 3. Therefore, the transient absorption spectrum at the fixed frequency offset of −40 cm^{-1} cannot distinguish the two tier populations. However, the continued time evolution of the spectral line shape supports the tier model for IVR.

The transient absorption signals at the frequency of the acetylenic C−H stretch fundamental and at −40 cm^{-1} for seven terminal acetylenes are shown in Figure 5. These measurements show the expected features. The decay is biexponential with time constants that match those determined in the excited-state absorption measurement. However, because the slower energy flow into the second tier contributes to both the SEP and bleach-recovery terms, the amplitude of the slow component is enhanced relative to that of the fast component when the spectrum is measured at the C−H stretch fundamental frequency (Table 6). Also, the bleach is not fully recovered in the gas phase because the absorption spectrum of molecules in the excited state is broadened and shifted (Figure 4). As the population is transferred from the acetylenic C−H stretch to the vibrational state with 2 quanta in the acetylenic C−H bend during the initial relaxation process as shown with the tier model, the amount of signal that is not recovered in the $v = 0-v = 1$ measurement can be found in the −40-cm^{-1} measurement.

For two of the terminal acetylenes in this study (propargyl fluoride and TMSA), the decay of the excited-state population is well described using a single time constant. Transient absorption at the characteristic frequency of vibrational states with C−H bend overtone excitation is observed for propargyl fluoride. The rise time of this signal matches the decay time of the excited state as shown in Figure 5. TMSA has a slow IVR rate, and we do not observe noticeable transient absorption at the −40-cm^{-1} shifted probe frequency, which suggests that the

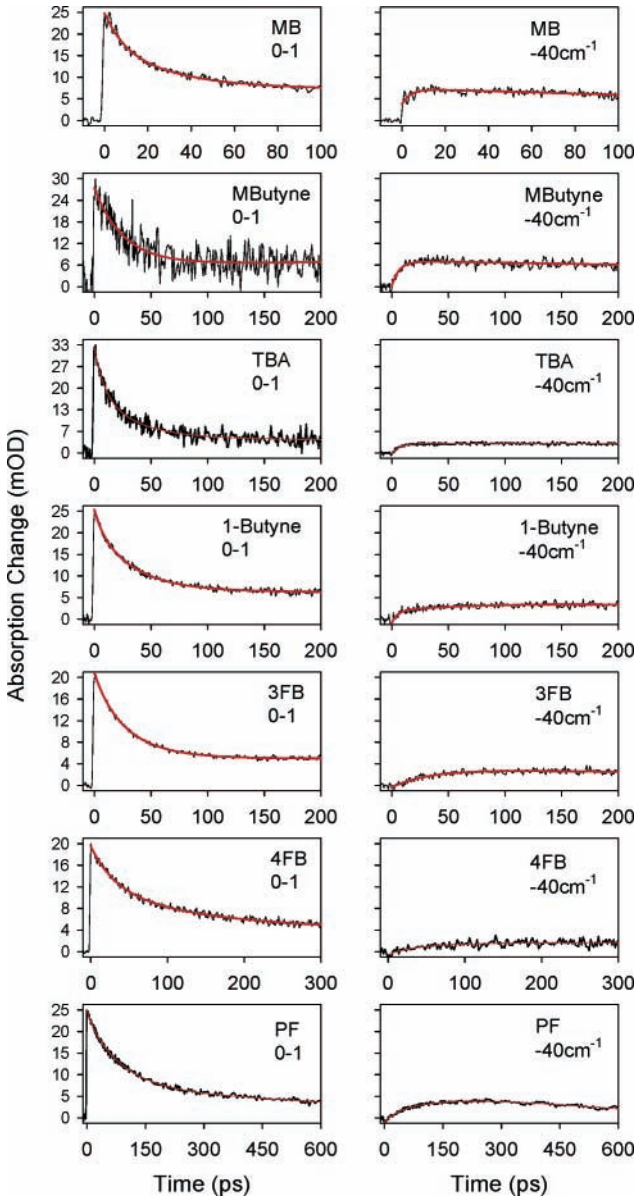

Figure 5. Transient absorption spectra measured by probing the C−H stretch frequency fundamental and −40 cm^{-1} from the fundamental frequency (the acetylenic C−H bend overtone states). The decay of the $v = 0 - v = 1$ probed signal is biexponential with about the same two time constants as the ones observed in the $v = 1 - v = 2$ measurement. The relative amplitude of the slow component compared to that of the fast component is enhanced in this measurement compared to the signal at the $v = 1 - v = 2$ frequency (Table 6). As population is transferred from the acetylenic C−H stretch to the vibrational state with 2 quanta in the acetylenic C−H bend during the initial relaxation process as shown with the tier model, the amount of signal that is not recovered in the $v = 0 - v = 1$ measurement can be found in the −40-cm^{-1} measurement. The signal is not fully recovered because the absorption spectrum of the molecule near these frequencies is broadened and shifted by the IVR process (Figure 4).

IVR pathway for TMSA does not involve vibrational states with C−H bend overtone excitation.

For propyne, which has a fast, small amplitude decay for the excited state (32 ps) followed by a slow decay consistent with collisional relaxation time scales (500 ps), we observe no absorption at the −40-cm^{-1} shifted probe position. Although this result suggests that the bend overtone states are not involved in the dynamics, the low sensitivity for this measurement makes it impossible to rule out this IVR pathway. In fact, transient absorption at the bend overtone frequency appears on the IVR time scale (22 ps) in dilute solution, suggesting that the initial IVR process of propyne does involve population transfer to vibrational states with bend overtone excitation.

For propargyl chloride, we observe a slow population relaxation time scale (380 ps) in both of the absorption signals at both the $v = 1 - v = 2$ position and the C−H stretch fundamental. No transient absorption is observed in the region of the bend overtone states. The analysis results of all 10 terminal acetylenes at the different probe positions are presented in Table 6.

Finally, we consider the issue of the competition between the relaxation of C−H into the first-tier vibrational states (with bend overtone excitation) and the dense set of second-tier states (all other vibrational states that lack the unique spectral signature of vibrational states with bend overtone excitation). The initial population decay rate of the C−H stretch is the sum of these two pathways. However, they affect the bleach-recovery measurement differently. If relaxation into the first-tier dominates the initial IVR process, then the amplitude of the fast component of the biexponential signal in the bleach-recovery measurement will be half as large as the amplitude in the decay of the C−H stretch excited-state absorption. This factor comes from the vibrational dependence of the transition dipole moment in the harmonic oscillator limit. In the opposite limit, where the relaxation rate to the second tier is dominant, biexponential signals would not be observed at either the excited state or C−H stretch fundamental frequencies. A quantitative determination of the relative rates of these processes for cases intermediate between these two limits requires an accurate determination of the amplitudes for the fast and slow rate contributions. In practice, we find that the current experiments lack sufficient amplitude reproducibility to quantitate the competition between the two pathways. For example, in five separate measurements for butyne, the amplitude ratio of the fast component in the bleach-recovery and C−H excited-state measurements is 0.54-(0.26). The uncertainty in this number is large, but the closeness of this ratio to the limiting value of 0.5 suggests that the relaxation rate to the first-tier states dominates the IVR pathway for the terminal acetylenes.

Discussion

In the previous paper, we showed that the total relaxation rate in solution of the first excited state of the acetylenic C−H stretch can be quantitatively described as the sum of a molecule-dependent IVR rate (obtained from the gas-phase measurement) and a solvent-dependent VER rate. For each solvent, a single VER rate is sufficient to account for the solvent enhancement of the relaxation rate for all terminal acetylenes. These results are consistent with a simple model for solvent relaxation where IVR and VER act independently:[11,23]

$$k_{TOT} = k_{IVR} + k_{VER} \quad (1)$$

In this paper, we have shown that the isolated-molecule dynamics for several terminal acetylenes occur on two distinct time scales. The initial population redistribution involves near-resonant vibrational states with 2 quanta of the acetylenic C−H bend. A second IVR time scale that is about 5 times slower and corresponds to further population redistribution into other vibrational modes of the molecule can also be identified. The goal of the analysis in this section is to determine whether the

TABLE 6: Lifetimes (ps) of the Acetylenic C−H Stretch at Room Temperature in the Gas Phase (Also Relative Amplitudes) by Probing at the Fundamental Frequency Listed along with the Values Measured at the $\nu = 1-\nu = 2$ Probe Frequency[a]

molecule	τ_1 (1−2)	τ_2 (1−2)[b]	A_2/A_1 (1−2)	τ_1 (0−1)	τ_2 (0−1)[b]	A_2/A_1 (0−1)	τ_{rise} (−40 cm^{-1})[c]
H−C≡CCH$_3$	32(3.2)	520(52)		28(5.8)	470(240)		
H−C≡CCH$_2$F	89(8.9)			77(10)			79(70)
H−C≡CCH$_2$Cl	380(70)			390(180)			
H−C≡CCH$_2$CH$_3$	8.3(1.0)	44(4.4)	1.9	8.3(1.6)	37(5.9)	3.1	9.4(1.2)
H−C≡CC(CH$_3$)=CH$_2$	4.0(0.6)	23(6.0)	1.5	5.9(1.0)	20(2.4)	2.1	3.0(1.1)
H−C≡CCH(CH$_3$)$_2$	5.6(1.0)	25(5.0)	1.5	5.4(4.9)	33(4.6)	2.9	5.1(1.1)
H−C≡CCHFCH$_3$	22(5.8)	52(14)	0.5	13(6.2)	31(3.1)	4.9	33(3.3)
H−C≡CCH$_2$CH$_2$F	34(3.4)	140(20)	1.0	34(11)	210(190)	1.1	37(12)
H−C≡CC(CH$_3$)$_3$	5.9(1.0)	39(3.9)	2.2	7.8(2.5)	30(20)	3.0	6.1(4.6)
H−C≡CSi(CH$_3$)$_3$	96(9.6)			96(16)			

[a] Also listed are time scales (ps) of bend overtone state rise rates in at room temperature in the gas phase probed −40 cm^{-1} from the acetylenic C−H stretch fundamental frequency. Uncertainties are shown in parentheses. [b] Three molecules do not require the second time constant for the exponential fit to the decay spectrum, and no τ_2 values are reported for those molecules. [c] We do not observe the population rise of the C−H bend overtone states, within our current signal-to-noise ratio, for three molecules, hence no lifetimes are reported.

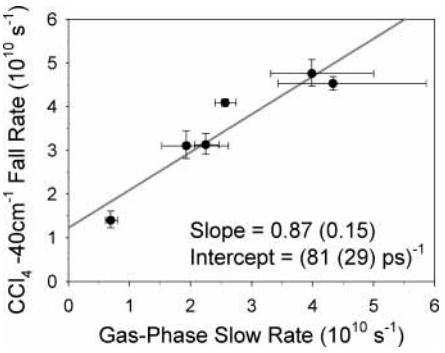

Figure 6. Solution rate plotted against the IVR rate for the second part of the relaxation process. For the relaxation rate of the intermediate state in solution, the same analysis used for the initial relaxation rate is applied, where the total relaxation rate is the sum of the IVR and VER rates. A linear relationship is also observed, indicating that the VER contribution to the second step is also constant for all of the molecules. The lifetime of the VER contribution to the second stage of the relaxation process in CCl_4 solution is 81(29) ps. The observation of a slope of ~1 (0.87(0.15)) indicates that the IVR rate of the first-tier states is the same for the isolated and solvated molecules.

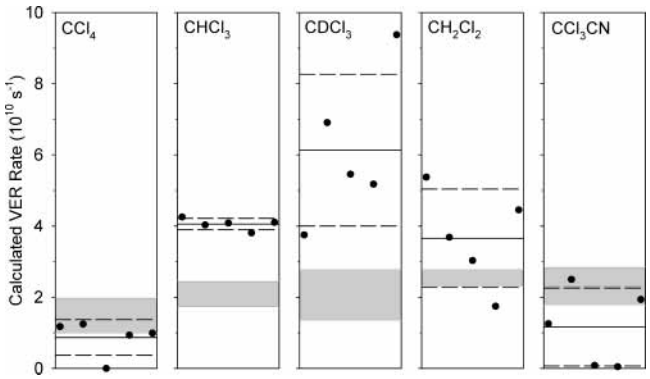

Figure 7. The VER rate for the second stage of the relaxation is compared to the VER rate for the first stage for each solvent using five molecules: butyne, 3-fluorobutyne, methylbutenyne, methylbutyne, and tertbutylacetylene, which are shown from the left-to-right in each panel. The average value and the standard deviation for the second-step VER rate are shown as horizontal reference lines. A shaded rectangle shows the acetylenic C−H stretch VER rate (intercept in Figures 2 and 4 of ref 11), where the error estimate of the C−H stretch VER rate is indicated as the width of the rectangle.

simple model expressed by eq 1 remains valid for the second, slower IVR step.

Using the same analysis as in the previous paper, we compare the isolated-molecule IVR rate for the slower population-redistribution step to the secondary total relaxation rate measured in dilute CCl_4 solution in Figure 6. For the slower relaxation time scale, we observe a linear relationship between the isolated molecule and solution rates in accord with eq 1. From the linear regression analysis, we determine that the VER rate of vibrational states with overtone excitation of the C−H bend in CCl_4 is 81(29) ps. This VER contribution is the same for all six of the terminal acetylenes in this study where we have been able to identify a hierarchical IVR process. The slope of the plot is 0.87(0.15). Within the uncertainty of the data, the purely intramolecular time scale for the second stage of IVR is unaffected by the solvent. (This behavior would produce a slope of 1.)

We take a slightly different approach to analyzing the data for the other four solvents in this study. For these systems, we determine the VER contribution to the slower stage of population relaxation for five molecules of the molecules with two identifiable IVR time scales. In this analysis, we exclude one of the molecules (4-fluorobutyne) that appear in Figure 6. This molecule is omitted because the IVR time scale for the fast redistribution process is 35 ps. In the previous paper, we showed that the VER contribution to the solution-phase relaxation rate is about 40−50 ps for the remaining solvents. Therefore, the solvent-relaxation pathway makes a large contribution to the initial relaxation in 4-fluorobutyne and can, therefore, modify the relaxation pathway from the purely intramolecular result.

The value for the VER rate (k_{VER}) is calculated using eq 1 and the slower IVR rate of the isolated molecule (k_{IVR}). Two determinations of the total solution relaxation rate (k_{TOT}) are possible with the data set. This rate can be obtained from either the decay of the acetylenic C−H bend overtone state absorption signal or the slow component of the bleach-recovery signal. The average of these two determinations is used, when both values are available, to obtain k_{VER} from eq 1. For each of the five terminal acetylenes, the VER rate for the second stage of IVR is compared to the VER rate for the C−H stretch in the scatter plots of Figure 7. The shaded rectangle gives the VER rate for the C−H stretch and is obtained from the intercept of each line in Figures 2 and 4 of ref 11. The width of the shaded box is determined from the error estimate of the intercept in the linear least-squares fit.

Although the current data set is limited to only five molecules, the expectations of eq 1 are found. For each of the five solvents, we observe a VER rate that is approximately constant for all of the terminal acetylenes. The spread of VER rates around the average is on the order of the measurement uncertainties (±1

TABLE 7: VER Lifetimes (ps) for the First and Second Stages of the Relaxation Process in Solution[a]

solvent	τ_{VER1}	τ_{VER2}
CCl_4	67(22)	93(13)[b]
$CHCl_3$	48(8.3)	25(1.0)
$CDCl_3$	48(17)	16(5.7)
CH_2Cl_2	39(3.6)	27(10)
CCl_3CN	43(10)	86(82)

[a] Uncertainties are shown in parentheses. [a] We obtained a lifetime of 81(29) ps for the second stage of VER in CCl_4 as described in Figure 6. These lifetime values are the same within the uncertainties.

$\times 10^{10}$ s^{-1}, Figure 7). Even though there is a range of VER rates in a single solvent, systematic differences in the VER contribution for each solvent are observed. The average VER rate at the second stage of IVR in each solvent that is obtained from the present analysis is reported in Table 7. Systematic differences in the solvent-induced vibrational-energy relaxation rate at the different stages of IVR are also observed. In particular, the VER rate for the second IVR process is faster than the C−H stretch VER for $CHCl_3$ and $CDCl_3$. The opposite behavior is found for CCl_3CN, where slower VER occurs for the relaxation of the first tier.

Although the rates of the intramolecular processes appear to be preserved in solution, solvation clearly affects the dynamics. As noted in the previous work, the decay of the excited-state population in solution is single-exponential, not biexponential as found for the isolated molecule. For the terminal acetylenes where the IVR rate for the first-tier redistribution step exceeds the VER rate, the solution-relaxation rate is equal to the intramolecular rate. However, the extent of population transfer to the first tier is enhanced in solution, allowing the complete relaxation of the C−H stretch population. In a future publication, we will show that this effect can be caused by solvent interactions that would be termed purely dephasing (T_2*) in the normal-mode basis set.[77]

The second obvious difference between the gas-phase and solution-phase results is that the bleach recovery returns to the baseline in solution on the relaxation time scale of the vibrational states with 2 quanta of the C−H bend. As will be shown in a future publication that analyzes the gas-phase "hot-molecule" spectrum (i.e., the long-time limit in Figure 3), much of the broadening and shifting of the fully relaxed molecule can be attributed to excitation in the low-frequency acetylene wag normal modes.[78] Other than the C−H bend, these are the only normal modes that cause an appreciable shift in the C−H stretch vibrational frequency.[11] Therefore, the observation of a return to baseline absorption in the solution-phase bleach-recovery experiment implies that vibrational energy is rapidly removed from the acetylenic wag normal modes by the solvent. The vibrational frequencies for these modes are in the 150−350 cm^{-1} range and lie in the characteristic frequency range of the solvent bath motions.[79−81] On the basis of many studies of vibrational relaxation in solution, it is reasonable to expect that the energy in these modes is rapidly cooled by the solvent.

To conclude our analysis of the vibrational dynamics of terminal acetylenes, we summarize our results graphically in Figure 8. This figure shows the measured total relaxation rates in solution for each of the steps in the relaxation pathway. These measured values are shown for the four terminal acetylenes with fast IVR for both steps. For each molecule, the solution-phase rates are shown for the five solvents in our study. Also, for each of the relaxation stages we include a molecule where no IVR contribution to the relaxation is expected. For the initial relaxation of the C−H stretch, this "baseline" molecule is propargyl chloride where exceptionally slow relaxation is observed in the gas phase so that the total relaxation rate in solution is dominated by the solvent VER contribution. For the second stage of the relaxation process, we choose propyne as the baseline system. A fast initial relaxation of the C−H stretch is observed in the gas phase for propyne. Furthermore, a strong transient absorption signal at the frequency of vibrational states with bend overtone excitation is found in solution. The rise time of this signal is consistent with this step having an intramolecular origin (i.e., eq 1 quantitatively predicts the rise time). However, because propyne is small, there is no dense bath present for the second stage of IVR, so k_{IVR} is expected to be zero for this step. The solution-phase rates calculated using eq 1 and the data in Tables 6 and 7 are also shown for each molecule. For the "reference molecules", the total solution relaxation rate calculated from eq 1 is just k_{VER} ($k_{IVR} = 0$). The simple model where

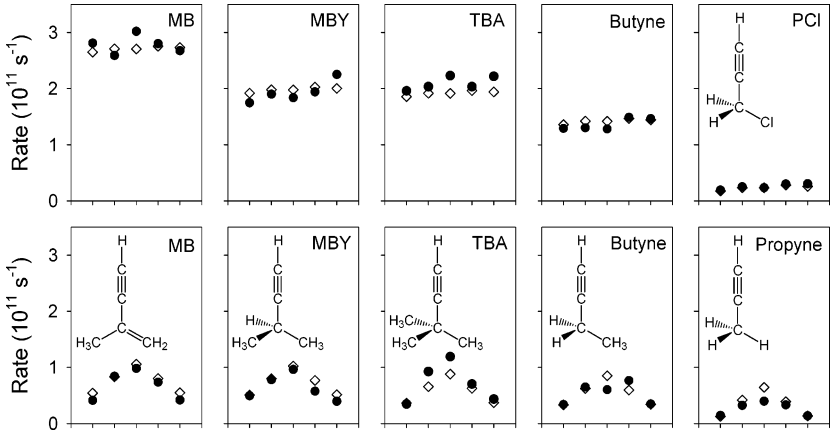

Figure 8. The measured solution rate (●) is compared to the calculated rate using eq 1 (◇) for each stage of the relaxation process in solution. The panels in the top row show the total relaxation rate for the excited state of the acetylenic C−H stretch, and the bottom-row panels show the relaxation rate of the vibrational states with the C−H bend overtone excitation. For each molecule, the solution-phase rates are shown for the five solvents in our study: CCl_4, $CHCl_3$, $CDCl_3$, CH_2Cl_2, and CCl_3CN (from left to right in each panel). The magnitude of the total relaxation rate for each molecule can be compared to the rate of the baseline molecule (propargyl chloride for the first stage and propyne for the second step, where $k_{IVR} \approx 0$). The difference between the measured rate and the "baseline" rate comes from the molecule-dependent IVR contribution to the total rate in solution. The different solvent "patterns" (linear vs wedged shape) in the two stages of the relaxation process show that the VER process depends on the nature of the vibrational motion.

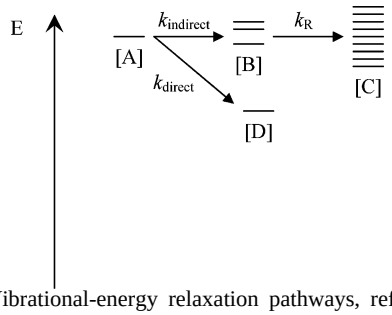

Figure A1. Vibrational-energy relaxation pathways, referred to as "direct" and "indirect" in this model. The direct path leads to vibrational states that absorb light within the laser bandwidth of the C−H stretch fundamental, and the indirect pathway leads to the vibrational states with the C−H bend overtone excitation (no absorption at the C−H stretch fundamental frequency). The indirect path is often called the bottleneck to the relaxation because it causes a delay in recovery of the absorption signal at the fundamental frequency.

IVR and VER proceed independently (and a single VER rate describes the behavior of all terminal acetylenes) can quantitatively explain the full set of measured solution-phase rates. This representation of the data also provides a clear illustration of the qualitatively different solvent effects in the two stages of relaxation dynamics through the different "solvent patterns" seen for the C−H stretch and first-tier relaxation.

Conclusions

Picosecond transient absorption spectroscopy techniques originally developed for solution-phase experiments have been successfully applied to gas-phase samples. The use of time-domain spectroscopy techniques has provided a powerful tool for assigning the pathway for vibrational energy relaxation following mode-specific excitation in isolated molecules. In this work, we exploited an unusual feature of the vibrational

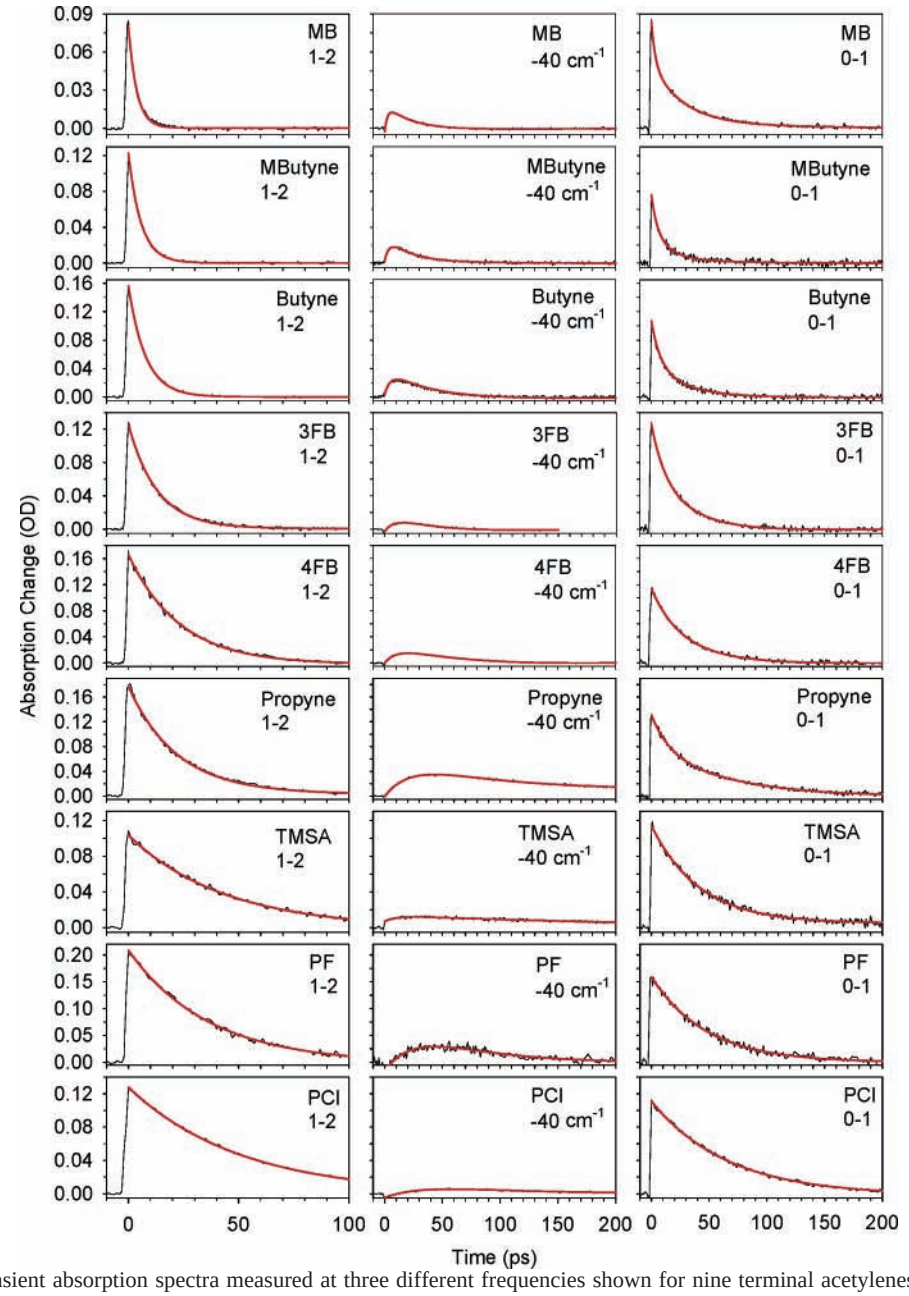

Figure A2. Three transient absorption spectra measured at three different frequencies shown for nine terminal acetylenes in dilute CCl_4 solution at room temperature. Each molecule is probed at the excited-state absorption frequency (1−2 measurement, $\Delta\nu = -105$ cm^{-1}), at the fundamental frequency (0−1 measurement), and 40 cm^{-1} down from the fundamental frequency (−40-cm^{-1} measurement, the C−H bend overtone state) following coherent excitation of the acetylenic C−H stretch fundamental. The exponential fit to each spectrum is shown by a red line (single-exponential for the 1−2 measurement and biexponential for both the 0−1 and −40-cm^{-1} measurements).

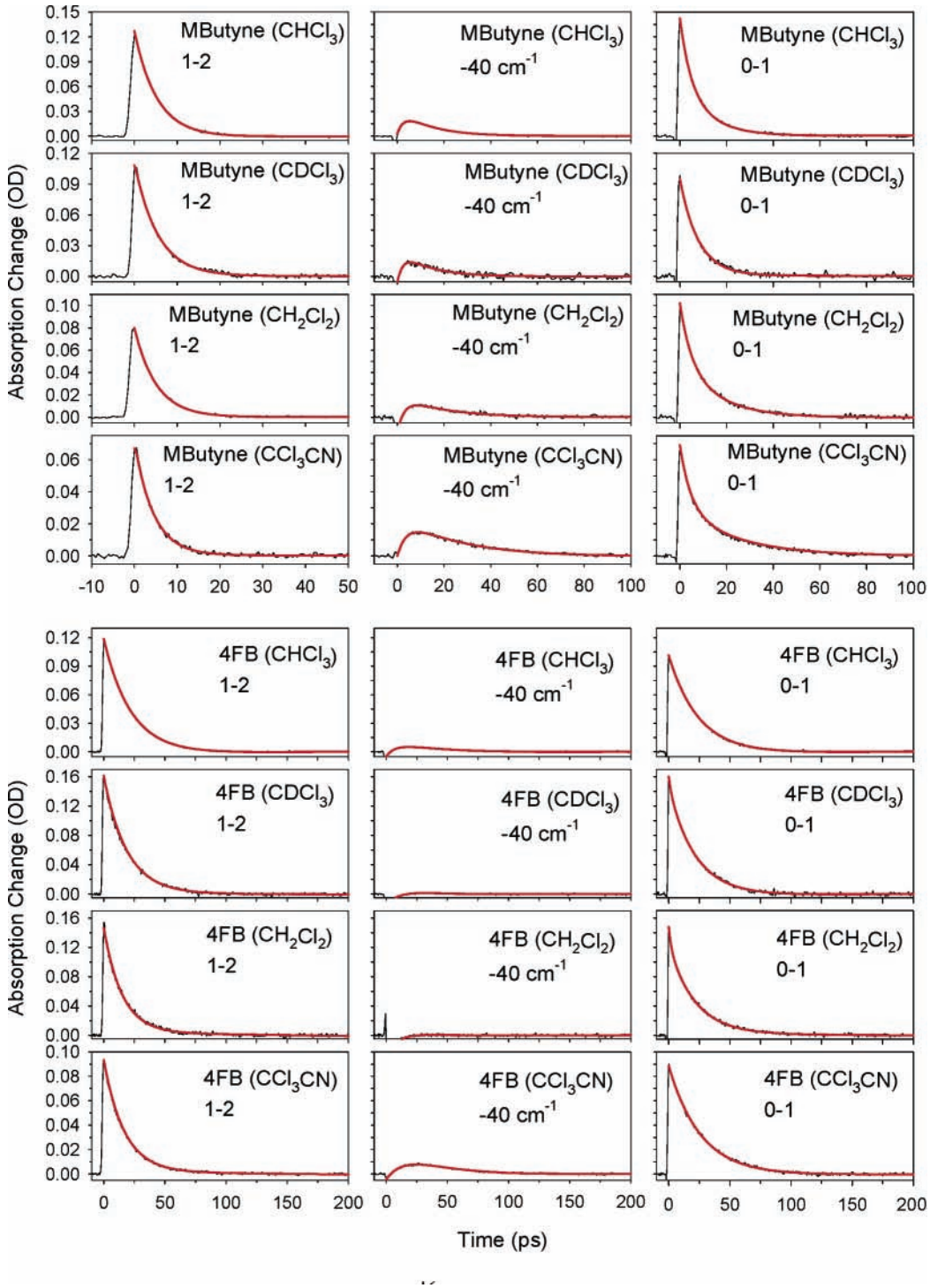

Figure A3. Three transient absorption spectra for 2 of 10 terminal acetylenes in 4 other CCl_4-like solvents. We show methylbutyne (fast initial IVR molecule) and 4-fluorobutyne (slow initial IVR molecule). These spectra were taken the same way as the ones described in Figure A2.

spectroscopy of terminal acetylenes: the large off-diagonal anharmonicity between the C−H stretch and C−H bend. The large shift in the C−H stretch absorption frequency for vibrational states with 2 quanta of C−H bend excitation allowed us to show unambiguously that the fast initial relaxation process in the gas phase involves population transfer from the first excited state of the acetylenic C−H stretch (3330 cm^{-1}) into vibrational combination bands with 2 quanta of the acetylenic C−H bend (about 1250 cm^{-1} of vibrational energy) and excitation in other lower-frequency vibrational modes (with the remaining ~2000 cm^{-1} of vibrational energy distributed in these modes). In this way, the vibrational dynamics of the C−H stretch of terminal acetylenes fall into the general class of stretch−bend dynamics that have been found to control the early-time dynamics of many other C−H stretch systems.[2,3,5,6] The next stage of the IVR process, where the full excitation energy is redistributed throughout the molecule, has a molecule-dependent rate. However, we find that the ratio of the rates for the two IVR steps is approximately the same for all terminal acetylenes. The mechanistic origin for the near-constant ratio of the two time scales remains to be understood.

The newly gained understanding of the purely intramolecular dynamics of the terminal acetylenes has paved the way for the study of solvent effects in vibrational-energy relaxation. The

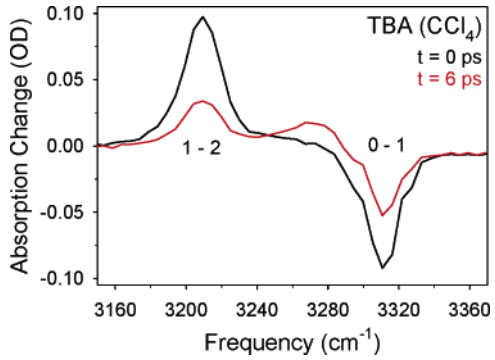

Figure A4. Transient absorption spectra of TBA in CCl_4 solution taken at two different delay times: at $t = 0$ and at $^1/_e$ time of the IVR decay. A sharp absorption feature appears at the frequency region of the C−H bend overtone excitation (−40 cm^{-1}), indicating that the indirect path is favored during the relaxation process of the C−H stretch excited state. The general shape of this feature is similar to that of the C−H stretch excited-state absorption, and we assume that the cross sections for these vibrational states are the same as the fundamental cross section.

direct correlation of the total relaxation rate in dilute solution with the isolated molecule rate for both stages of the IVR process shows that the solvent effect makes a simple additive contribution to the relaxation processes in terminal acetylenes. The VER and IVR processes contribute independently to the vibrational dynamics. For dilute solutions, the solvent VER contributions to the relaxation rate of the acetylenic C−H stretch and the first-tier states that contain C−H bend overtone excitation are different depending on the nature of the solvent. The problem of "solvent effects" in vibrational relaxation acquires a new richness when relaxation pathways are considered.

For several of the molecules in this study, the time scales of isolated-molecule IVR are significantly faster than the solvent VER rate. A theoretical understanding of solvent-induced vibrational-energy relaxation cannot be based on the usual assumption of the excitation of a stationary state of the vibrational Hamiltonian in these cases.[37,79−86] Incorporating the time-dependent vibrational dynamics from the purely intramolecular process into solution-phase energy relaxation theories presents a new challenge to the field.

Acknowledgment. We thank John Keske and Frances Rees for their help with the terminal acetylene sample set. This work was supported by the Chemistry Division of the National Science Foundation (CHE-0078825) and the Optical Sciences and Engineering Division of the National Science Foundation. Additional support for this work came from the SELIM Program and the AEP Program at the University of Virginia.

Appendix A: Dilute CCl_4 Solution Measurements

The basic kinetics model for vibrational-energy relaxation in the solution phase needs to take into account that the infrared spectrum can distinguish between a direct-energy relaxation pathway into vibrational states that absorb light at the C−H stretch fundamental frequency and an indirect relaxation pathway via a vibrational state with 2 quanta of the acetylenic C−H bend. The kinetics model for interpreting the three transient absorption spectra is shown in Figure A1. The "species" in this model are groups of vibrational states that have the same absorption spectrum. Species A is the C−H stretch excited state (−105-cm^{-1} absorption frequency), B collects all vibrational states with 2 quanta of the C−H bend (−40-cm^{-1} absorption frequency), and C and D correspond to the vibrational states that absorb within the laser bandwidth of the C−H stretch fundamental. This model is similar to the one used in the previous paper where two processes, IVR and VER, contributed to the total relaxation rate in solution.[11] However, it is not proper to associate the two pathways in Figure A1 with the IVR and VER processes. Instead, both the IVR and VER pathways follow the dynamics of the model in Figure A1. This kinetics model has been employed in previous experiments, and the indirect path is often called the bottleneck to relaxation because it causes a delay in the recovery of absorption at the frequency of the fundamental.[68,69]

The time-dependent populations of the different groups of vibrational states can be determined analytically and, using the notation in the figure, are

$$[\mathrm{A}](t) = \exp(-(k_{\mathrm{indirect}} + k_{\mathrm{direct}}) \cdot t) \tag{A1}$$

$$[\mathrm{B}](t) = \left(\frac{k_{\mathrm{indirect}}}{k_{\mathrm{R}} - (k_{\mathrm{indirect}} + k_{\mathrm{direct}})}\right) \cdot [\exp(-(k_{\mathrm{indirect}} + k_{\mathrm{direct}}) \cdot t) - \exp(-k_{\mathrm{R}} \cdot t)] \tag{A2}$$

$$[\mathrm{C}](t) = -k_{\mathrm{indirect}} \cdot \left[\left(\frac{1}{k_{\mathrm{indirect}} + k_{\mathrm{direct}}} + \frac{1}{k_{\mathrm{R}} - (k_{\mathrm{indirect}} + k_{\mathrm{direct}})}\right) \cdot \exp(-(k_{\mathrm{indirect}} + k_{\mathrm{direct}}) \cdot t)\right] + \left(1 - \frac{k_{\mathrm{direct}}}{k_{\mathrm{indirect}} + k_{\mathrm{direct}}}\right) + \frac{k_{\mathrm{indirect}}}{k_{\mathrm{R}} - (k_{\mathrm{indirect}} + k_{\mathrm{direct}})} \cdot \exp(-k_{\mathrm{R}} \cdot t) \tag{A3}$$

$$[\mathrm{D}](t) = \frac{k_{\mathrm{direct}}}{k_{\mathrm{indirect}} + k_{\mathrm{direct}}} \cdot [1 - \exp(-(k_{\mathrm{indirect}} + k_{\mathrm{direct}}) \cdot t)] \tag{A4}$$

For two of the measurements, the transient absorption signals are easily related to the populations in the kinetics model: the excited-state absorption directly reflects the kinetics of the acetylenic C−H stretch (labeled A), and the absorption shifted by −40 cm^{-1} is proportional to the population of vibrational states with 2 quanta of C−H bend excitation (labeled B). The bleach-recovery signal is comparatively more complicated because it includes both the SEP contribution (the acetylenic C−H stretch, A) and the absorption recovery (from the group of vibrational states C and D that have "unshifted" C−H stretch absoprtions). The functional forms for the three transient absorption signals, which include a relative absorption cross section for each set of vibrational states, are

excited-state $v = 1 - v = 2$ absorption:

$$\mathrm{signal}(t) = 2\sigma_{\mathrm{CH}}[\mathrm{A}](t) \tag{A5}$$

bend overtone absorption:

$$\mathrm{signal}(t) = \sigma_{\mathrm{B}}[\mathrm{B}](t) \tag{A6}$$

C−H fundamental absorption:

$$\mathrm{signal}(t) = \{\sigma_{\mathrm{CH}}(1 - [\mathrm{A}](t))\} + \{\sigma_{\mathrm{C}}[\mathrm{C}](t) + \sigma_{\mathrm{D}}[\mathrm{D}](t)\} \tag{A7}$$

The excited-state absorption signal, eq A5, decays with a single time constant given by the sum of the direct and indirect relaxation rates. (The factor of 2 in the prefactor comes from the harmonic oscillator vibrational transition strength.) The

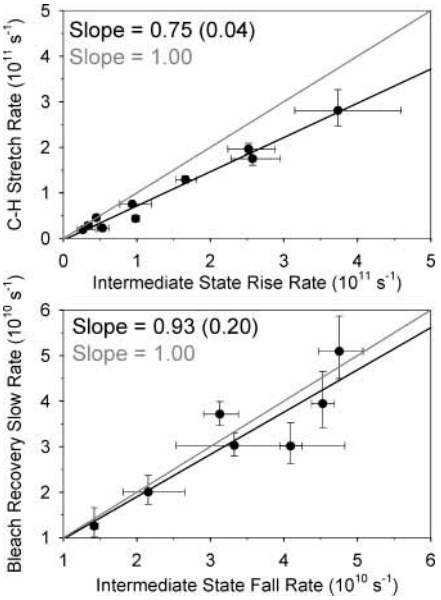

Figure A5. Relationships among the relaxation rates in CCl_4 solution obtained at three different probe frequencies. The excited-state relaxation rate (both the single time constant of the $v = 1-v = 2$ measurement and the fast time constant of the bleach-recovery measurement) matches the rise time of the C−H bend overtone states (top panel), and the slow time scale of the bleach recovery matches the fall time of the C−H bend overtone states (bottom panel). As expected, the correlations are good among the rates measured at three different probing frequencies. One deviation from the model is that the total relaxation rate measured by the rise of the C−H bend overtone excitation is faster than the rate measured by the decay of the excited-state absorption.

absorption spectrum in the region for vibrational states with overtone bend excitation, which is the intermediate for the indirect path, has a biexponential form, eq A6. One time constant is the total relaxation rate of the excited state; the other is the rate at which the bend overtone states relax to vibrational states that reabsorb at the fundamental frequency. The bleach-recovery signal, eq A7, is also biexponential in this model, with the same two time constants observed for the intermediate.

The analysis of the three transient absorption measurements using eqs A5−A7 is shown in Figure A2 for nine of the terminal acetylenes in CCl_4. (The results for TBA are shown in Figure 1.) The transient absorption spectra in the different solvents used in this study are shown for two of the terminal acetylenes in Figure A3. By relaxing through the indirect pathway, the bleach-recovery signal attains a biexponential form with the same time constants observed for the population of C−H bend overtone intermediate states. The spectra of Figures A2 and A3 are consistent with this conclusion. For example, the previous paper showed that the relaxation of the C−H stretch is dominated by IVR for TBA. In solution, the vibrational states with $v = 2$ of bend excitation decay on a time scale of ∼30 ps (Figure 1). This second time scale is in good agreement with the time scale assigned to relaxation into the second tier of states for the isolated molecule (39 ps, Figure 3).

It would be useful to quantify the relative relaxation rates of the indirect and direct pathways. Using experimental time constants alone, it is not possible to determine the relative rates of direct and indirect relaxation. This determination can be made only by using the amplitudes of the two rate contributions, and this information is less reliable. Furthermore, an accurate division of the total relaxation rate of the C−H stretch fundamental into the two contributions requires a knowledge of the relative absorption cross sections in eqs. A5−A7. It is difficult to predict the absorption cross section for the vibrational states with bend overtone excitation. One potential problem is that this absorption feature could be broadened by the excitation in other normal modes, leading to a reduced peak cross section in the experiment. To investigate these effects, we have measured the absorption spectrum of TBA in dilute CCl_4 solution at the two fixed time delays shown in Figure A4. At a delay of 6 ps, a sharp absorption feature at the bend overtone frequency is observed. The overall shape of this feature is close to that of the excited-state absorption of the C−H stretch ($t = 0$). Therefore, we have assumed that the cross sections for these vibrational states are the same as the fundamental. As in the similar analysis of the gas-phase data described in the main text, our attempts to carry out the analysis using this assumption have been unsuccessful because of the experimental uncertainties in the amplitude data. However, for butyne and TBA (our largest

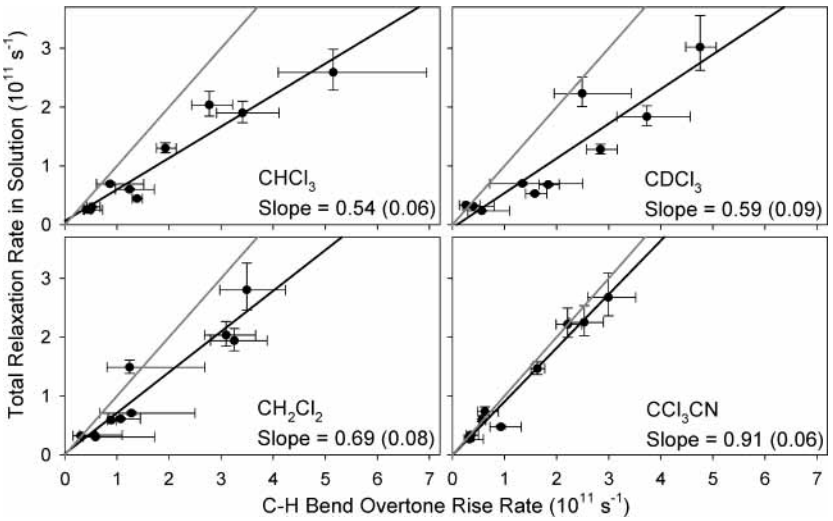

Figure A6. Total relaxation rate measured at the absorption frequency of the acetylenic C−H stretch excited state ($v = 1-v = 2$) plotted against the rise rate of the transient absorption signal for vibrational states with 2 quanta in the C−H bend (−40 cm^{-1}). As in the case of CCl_4 (Figure A5), the rise-time measurement is consistently faster than the relaxation rate of the excited-state absorption signal in all of the solvents. The gray line denotes a slope of 1 as a reference.

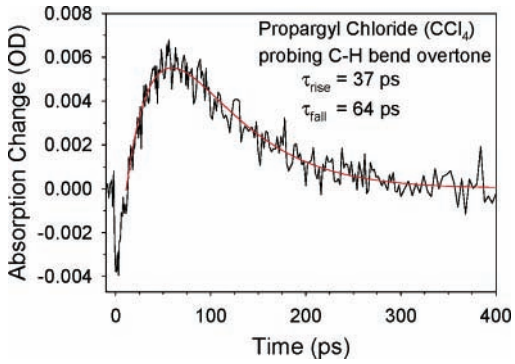

Figure A7. The transient absorption signal at the frequency region of the C−H bend overtone excitation is also observed for propargyl chloride in dilute CCl_4 solution. This molecule does not have IVR; therefore, this spectrum provides direct information about the VER dynamics for the terminal acetylenes in CCl_4 solution. As shown, the VER process directs some population transfer from the C−H stretch to the vibrational states with bend overtone excitation.

data sets), this analysis suggests that the indirect path proceeds at a rate that is 3−6 times faster than the direct relaxation pathway.

By measuring all three signals, we can check for internal consistency of the data. There are two sets of correlations that are expected in these measurements. The excited-state lifetime determination should match one of the two decay constants of the C−H bend overtone transient absorption spectrum and the fast component of the bleach-recovery measurement. The other decay constant for this transient absorption spectrum should match the slow component of the bleach-recovery signal. These correlations are shown in Figure A5 and behave as expected, except for one deviation. We find that the total relaxation rate measured by the rise of the C−H bend overtone absorption is consistently faster than the rate measured by the decay of the excited-state absorption. This effect cannot be accounted for by the model and suggests that some reversible energy transfer between the groups of states may be occurring.[21] As shown in Figure A6, this effect is observed in other solvents as well.

The analysis of the solution-phase spectra for propargyl chloride deserves special attention because the slow IVR rate observed in the gas phase means that the solvent-relaxation process (VER) will dominate the dynamics. There are two notable features of the results for this molecule. First, we still observed transient absorption in the spectral region of the bend overtone states (Figure A7). This result shows that the solution-relaxation process also favors energy transfer to vibrational states with bend excitation. This result supports much work on the C−H stretch VER process of other small molecules where the bend overtone receives population in the earliest stages of energy relaxation.[16,64,87−89] A second feature is that the lifetime measured in the excited-state absorption spectrum is shorter than the bleach-recovery lifetime, even though both can be quantitatively fit with a single decay time as shown in Figure A8. We have observed this behavior for other terminal acetylenes where the VER process makes a major contribution to the total relaxation rate (i.e., molecules with IVR lifetimes longer than the VER limit of ∼60 ps).

We find that this result is consistent with relaxation proceeding in part through the indirect path. We have attempted to determine the relative direct and indirect rates through the amplitudes of the transient absorption signal, but there are large uncertainties because the two time constants of the decay process are similar.[90] However, it appears that these channels have

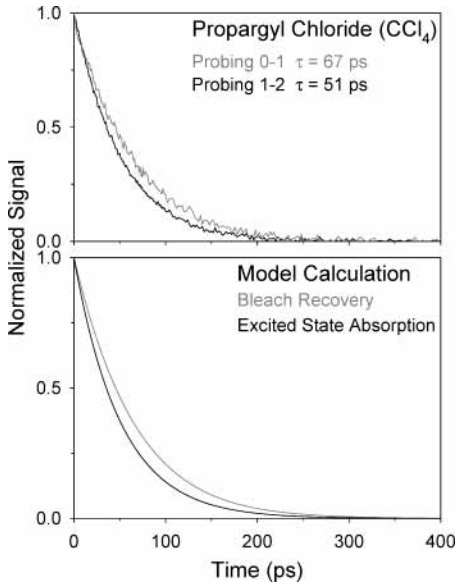

Figure A8. Excited-state absorption spectrum (probing $v = 1-v = 2$ of the acetylenic C−H stretch) compared to the bleach-recovery spectrum (the acetylenic C−H stretch fundamental frequency probe) for propargyl chloride in CCl_4 solution. Even though both results can be fit with a single-exponential expression, the bleach-recovery rate is slower than the rate observed in the excited-state absorption spectrum. Calculated signals are shown in the bottom panel. When direct and indirect rates are equal (both (102 ps)$^{-1}$), the bleach-recovery signal (eq A7) is single-exponential, but the rate determined by the bleach recovery is slower than the true relaxation rate, which is consistent with relaxation proceeding in part through the indirect pathway.

approximately equal rates. When equal direct and indirect rates are used in the model to account for the excited-state lifetime, the bleach-recovery signal predicted by eq A7 is single-exponential to high accuracy. However, the apparent rate determined by bleach recovery is slower than the true relaxation rate. The results from the kinetics model are also shown in Figure A8. From this analysis, we conclude that the VER process includes relaxation to vibrational states with bend overtone excitation, but this channel is not significantly faster than relaxation to vibrational states with 1 or no quanta of C−H bend excitation.

References and Notes

(1) Baer, T.; Hase, W. L. *Unimolecular Reaction Dynamics*; Oxford University Press: New York, 1996.
(2) Quack, M. *Jerusalem Symp. Quantum Chem. Biochem.* **1991**, *24*, 47.
(3) Pochert, J.; Quack, M.; Stohner, J.; Willeke, M. *J. Chem. Phys.* **2000**, *113*, 2719.
(4) Stuchebrukhov, A. A.; Kuzmin, M. V.; Bagratashvili, V. N.; Letokhov, V. S. *Chem. Phys.* **1986**, *107*, 429.
(5) Sibert, E. L.; Reinhardt, W. P.; Hynes, J. T. *J. Chem. Phys.* **1984**, *81*, 1115.
(6) Minehardt, T. J.; Wyatt, R. E. *J. Chem. Phys.* **1998**, *109*, 8330.
(7) Chapman, D.; Bowman, J. M.; Gazdy, B. *J. Chem. Phys.* **1992**, *96*, 1919.
(8) Nesbitt, D. J.; Field, R. W. *J. Phys. Chem.* **1996**, *100*, 12735.
(9) Lehmann, K. K.; Scoles, G.; Pate, B. H. *Annu. Rev. Phys. Chem.* **1994**, *45*, 241.
(10) Myers, D. J.; Shigeiwa, M.; Fayer, M. D.; Silbey, R. *Chem. Phys. Lett.* **1999**, *312*, 399.
(11) Yoo, H. S.; DeWitt, M. J.; Pate, B. H. *J. Phys. Chem. A* **2004**, *108*, 1348.
(12) Felker, P. M.; Lambert, W. R.; Zewail, A. H. *J. Chem. Phys.* **1985**, *82*, 3003.
(13) Baskin, J. S.; Banares, L.; Pedersen, S.; Zewail, A. H. *J. Phys. Chem.* **1996**, *100*, 11920.
(14) Owrutsky, J. C.; Raftery, D.; Hochstrasser, R. M. *Annu. Rev. Phys. Chem.* **1994**, *45*, 519.

(15) Heilweil, E. J.; Casassa, M. P.; Cavanagh, R. R.; Stephenson, J. C. *J. Chem. Phys.* **1986**, *85*, 5004.
(16) Bakker, H. J.; Planken, P. C. M.; Kuipers, L.; Lagendijk, A. *J. Chem. Phys.* **1991**, *94*, 1730.
(17) Iwaki, L. K.; Dlott, D. D. *Chem. Phys. Lett.* **2000**, *321*, 419.
(18) Seifert, G.; Zürl, R.; Graener, H. *J. Phys. Chem. A* **1999**, *103*, 10749.
(19) Urdahl, R. S.; Myers, D. J.; Rector, K. D.; Davis, P. H.; Cherayil, B. J.; Fayer, M. D. *J. Chem. Phys.* **1997**, *107*, 3747.
(20) Fendt, A.; Fischer, S. F.; Kaiser, W. *Chem. Phys. Lett.* **1981**, *82*, 350.
(21) Lim, M.; Hochstrasser, R. M. *J. Chem. Phys.* **2001**, *115*, 7629.
(22) Yoo, H. S.; McWhorter, D. A.; Pate, B. H. *J. Phys. Chem. A***2004**, *108*, 1380.
(23) Egorov, S. A.; Skinner, J. L. *J. Chem. Phys.* **2000**, *112*, 275.
(24) Bingemann, D.; King, A. M.; Crim, F. F. *J. Chem. Phys.* **2000**, *113*, 5018.
(25) Assmann, J.; Charvat, A.; Schwarzer, D.; Kappel, C.; Luther, K.; Abel, B. *J. Phys. Chem. A* **2002**, *106*, 5197.
(26) Rice, S. A. *Adv. Chem. Phys.* **1997**, *101*, 213.
(27) Demirplak, M.; Rice, S. A. *J. Chem. Phys.* **2002**, *116*, 8028.
(28) Sinha, A.; Hsiao, M. C.; Crim, F. F. *J. Chem. Phys.* **1990**, *92*, 6333.
(29) Thoemke, J. D.; Pfeiffer, J. M.; Metz, R. B.; Crim, F. F. *J. Phys. Chem.* **1995**, *99*, 13748.
(30) Crim, F. F. *Acc. Chem. Res.* **1999**, *32*, 877.
(31) Woods, E., III.; Cheatum, C. M.; Crim, F. F. *J. Chem. Phys.* **1999**, *111*, 5829.
(32) Bronikowski, M. J.; Simpson, W. R.; Girard, B.; Zare, R. N. *J. Chem. Phys.* **1991**, *95*, 8647.
(33) Guettler, R. D.; Jones, G. C.; Posey, L. A.; Zare, R. N. *Science* **1994**, *266*, 259.
(34) Poutsma, J. C.; Everest, M. A.; Flad, J. E.; Zare, R. N. *Appl. Phys. B* **2000**, *71*, 623.
(35) Kim, H. L.; Kulp, T. J.; McDonald, J. D. *J. Chem. Phys.* **1987**, *87*, 4376.
(36) Voth, G. A.; Hochstrasser, R. M. *J. Phys. Chem. A* **1996**, *100*, 13034.
(37) Stratt, R. M.; Maroncelli, M. *J. Phys. Chem.* **1996**, *100*, 12981.
(38) Shi, S.; Woody, A.; Rabitz, H. *J. Chem. Phys.* **1988**, *88*, 6870.
(39) Krause, J. L.; Shapiro, M.; Brumer, P. *J. Chem. Phys.* **1990**, *92*, 1126.
(40) Tannor, D. J.; Rice, S. A. *J. Chem. Phys.* **1985**, *83*, 5013.
(41) Colwell, S. M.; Jayatilaka, D.; Maslen, P. E.; Amos, R. D.; Handy, N. C. *Int. J. Quantum Chem.* **1991**, *40*, 179.
(42) Weinacht, T. C.; Bartels, R.; Backus, S.; Bucksbaum, P. H.; Pearson, B.; Geremia, J. M.; Rabitz, H.; Kapteyn, H. C.; Murnane, M. M. *Chem. Phys. Lett.* **2001**, *344*, 333.
(43) Assion, A.; Baumert, T.; Bergt, M.; Brixner, T.; Kiefer, B.; Seyfried, V.; Strehle, M.; Gerber, G. *Science* **1998**, *282*, 919.
(44) Levis, R. J.; Menkir, G. M.; Rabitz, H. *Science* **2001**, *292*, 709.
(45) Kosloff, R.; Rice, S. A.; Gaspard, P.; Tersigni, S.; Tannor, D. J. *Chem. Phys.* **1989**, *139*, 201.
(46) Kay, K. G.; Rice, S. A. *J. Chem. Phys.* **1972**, *57*, 3041.
(47) Heller, E. J.; Rice, S. A. *J. Chem. Phys.* **1974**, *61*, 936.
(48) Shore, B. W.; Johnson, M. A. *J. Chem. Phys.* **1978**, *68*, 5631.
(49) Ackerhalt, J. R.; Eberly, J. H. *Phys. Rev. A* **1976**, *14*, 1705.
(50) Shore, B. W. *The Theory of Coherent Atomic Excitation*; Wiley & Sons: New York, 1990; Vol. 2.
(51) Benmair, R. M. J.; Yogev, A. *Chem. Phys. Lett.* **1983**, *95*, 72.
(52) Lewis, F. D.; Teng, P. A.; Weitz, E. *J. Phys. Chem.* **1983**, *87*, 1666.
(53) Buechele, J. L.; Weitz, E.; Lewis, F. D. *J. Phys. Chem.* **1984**, *88*, 868.
(54) Coveleskie, R. A.; Dolson, D. A.; Moss, D. B.; Munchak, S. C.; Parmenter, C. S. *Chem. Phys.* **1985**, *96*, 191.
(55) Carey, F. A.; Sundberg, R. J. *Advanced Organic Chemistry*, part B; Plenum Press: New York, 1990.
(56) Davidsson, J.; Gutow, J. H.; Zare, R. N.; Hollenstein, H. A.; Marquardt, R. R.; Quack, M. *J. Phys. Chem.* **1991**, *95*, 1201.
(57) Pochert, J.; Quack, M. *Mol. Phys.* **1998**, *95*, 1055.
(58) Stuchebrukhov, A. A.; Marcus, R. A. *J. Chem. Phys.* **1993**, *98*, 6044.
(59) Stuchebrukhov, A. A.; Mehta, A.; Marcus, R. A. *J. Phys. Chem.* **1993**, *97*, 12491.
(60) Gottfried, N. H.; Zinth, W.; Kaiser, W. *J. Mol. Struct.* **1984**, *113*, 61.
(61) Graener, H.; Laubereau, A. *Appl. Phys. B* **1982**, *29*, 213.
(62) Hofmann, M.; Graener, H. *Chem. Phys.* **1996**, *206*, 129.
(63) Iwaki, L. K.; Dlott, D. D. *J. Phys. Chem. A* **2000**, *104*, 9101.
(64) Graener, H.; Zürl, R.; Hofmann, M. *J. Phys. Chem. B* **1997**, *101*, 1745.
(65) Dlott, D. D. *Chem. Phys.* **2001**, *266*, 149.
(66) Khalil, M.; Tokmakoff, A. *Chem. Phys.* **2001**, *266*, 213.
(67) Ebata, T.; Kayano, M.; Sato, S.; Mikami, N. *J. Phys. Chem. A* **2001**, *105*, 8623.
(68) Laubereau, A.; Kehl, G.; Kaiser, W. *Opt. Commun.* **1974**, *11*, 74.
(69) van den Broek, M. A. F. H.; Bakker, H. J. *Chem. Phys.* **2000**, *253*, 157.
(70) Yoo, H. S.; Rees, F. S.; Brown, G.; Douglass, K. O.; Johns, J.; Keske, J. C.; Nair, P.; Pate, B. H. Submitted.
(71) Pate, B. H. *J. Chem. Phys.* **1998**, *109*, 4396.
(72) Klots, C. E. *J. Chem. Phys.* **1989**, *90*, 4470.
(73) Gottfried, N. H.; Seilmeier, A.; Kaiser, W. *Chem. Phys. Lett.* **1984**, *111*, 326.
(74) Lokhman, V. N.; Petin, A. N.; Ryabov, E. A.; Letokhov, V. S. *J. Phys. Chem. A* **1999**, *103*, 11293.
(75) Lokhman, V. N.; Makarov, A. A.; Yu, I.; Ryabov, E. A.; Letokhov, V. S. *J. Phys. Chem. A* **1999**, *103*, 11299.
(76) Dübal, H.-R.; Quack, M. *Chem. Phys. Lett.* **1982**, *90*, 370.
(77) Yoo, H. S.; DeWitt, M. J.; Pate, B. H. In preparation.
(78) Yoo, H. S.; DeWitt, M. J.; Pate, B. H. In preparation.
(79) Grote, R. F.; van der Zwan, G.; Hynes, J. T. *J. Phys. Chem.* **1984**, *88*, 4676.
(80) Egorov, S. A.; Skinner, J. L. *J. Chem. Phys.* **1996**, *105*, 7047.
(81) Sibert, E. L.; Rey, R. *J. Chem. Phys.* **2002**, *116*, 237.
(82) Kenkre, V. M.; Tokmakoff, A.; Fayer, M. D. *J. Chem. Phys.* **1994**, *101*, 10618.
(83) Bakker, H. J. *J. Chem. Phys.* **1993**, *98*, 8496.
(84) Zinth, W.; Kolmeder, C.; Benna, B.; Irgens-Defregger, A.; Fischer, S. F.; Kaiser, W. *J. Chem. Phys.* **1983**, *78*, 3916.
(85) Bagchi, B.; Oxtoby, D. W. *J. Chem. Phys.* **1983**, *78*, 2735.
(86) Stratt, R. M. *Acc. Chem. Res.* **1995**, *28*, 201.
(87) Kolmeder, C.; Zinth, W.; Kaiser, W. *Chem. Phys. Lett.* **1982**, *91*, 323.
(88) Fendt, A.; Fischer, S. F.; Kaiser, W. *Chem. Phys.* **1981**, *57*, 55.
(89) Seifert, G.; Zürl, R.; Patzlaff, T.; Graener, H. *J. Chem. Phys.* **2000**, *112*, 6349.
(90) When these time constants are equal, the prefactor in eq 2 is undetermined.